

RESEARCH PAPER



## $\beta$ -hCG promotes epithelial ovarian cancer metastasis through ERK/MMP2 signaling pathway

Weimin Wu<sup>\*a</sup>, Hao Gao<sup>\*a</sup>, Xiaofeng Li<sup>\*a</sup>, Shumin Peng<sup>b</sup>, Jing Yu<sup>c</sup>, Na Liu<sup>a</sup>, Guangxi Zhan<sup>a</sup>, Yong Zhu<sup>d</sup>, Kai Wang<sup>e</sup>, and Xiaoqing Guo<sup>a</sup>

<sup>a</sup>Department of Obstetrics and Gynecology, Shanghai First Maternity and Infant Hospital, Tongji University School of Medicine, Shanghai, China; <sup>b</sup>Department of Obstetrics and Gynecology, Chongqing Health Center for Women and Children, Chongqing, China; <sup>c</sup>Department of Pathology, Shanghai First Maternity and Infant Hospital, Tongji University School of Medicine, Shanghai, China; <sup>d</sup>Department of Obstetrics and Gynecology, The First Affiliated Hospital, Shihezi University School of Medicine, Xinjiang, China; <sup>e</sup>Clinical and Translational Research Center, Shanghai First Maternity and Infant Hospital, Tongji University School of Medicine, Shanghai, China

### ABSTRACT

Epithelial ovarian cancer (EOC) is the most lethal gynecologic malignancy, with typically extensive intraperitoneal implantation leading to poor prognosis. Our previous study preliminarily demonstrated  $\beta$ -hCG can promote tumorigenesis in immortalized nontumorigenic ovarian epithelial cells. In this study, the roles and mechanisms of  $\beta$ -hCG in regulating EOC proliferation and metastasis were thoroughly explored. First, histologically,  $\beta$ -hCG was aberrantly overexpressed in human EOC metastatic tissues, and significantly correlated with FIGO stage, tumor size, differentiation, histologic grade and high grade serous ovarian carcinoma (HGSOC) ( $P < 0.05$ ). However, serologically,  $\beta$ -hCG expression showed no significant difference between EOC and nonmalignant ovarian patients. Second,  $\beta$ -hCG was confirmed to have no significant effects on EOC proliferation *in vitro* and *in vivo*, while  $\beta$ -hCG upregulation was proven to promote migration and invasion ability in ES-2 and OVCAR-3 cells *in vitro* ( $P < 0.05$ ), and  $\beta$ -hCG downregulation in SKOV3 cells had the opposite effect. Moreover, more invadopodia protrusions, mitochondria accumulations and cytoskeletal rearrangements were observed in  $\beta$ -hCG-overexpressing ES-2 cells, while  $\beta$ -hCG-depleted SKOV3 cells produced the opposite effect. Furthermore,  $\beta$ -hCG was confirmed to clearly facilitate intraperitoneal metastasis in nude mouse orthotopic ovarian xenograft models. Importantly, these effects of  $\beta$ -hCG were mediated by activation of the ERK/MMP2 signaling pathway, independently of luteinizing hormone/chorionic gonadotropin receptor (LHCGR) presence, and inhibition the pathway with the p-ERK1/2 inhibitor SCH772984 significantly impaired the tumor-promoting effects induced by  $\beta$ -hCG. Collectively, these data provide new insight into the roles and mechanisms of  $\beta$ -hCG in regulating EOC metastasis through ERK/MMP2 signaling pathway and may become a new target for therapeutic intervention.

### ARTICLE HISTORY

Received 11 July 2018  
Revised 16 November 2018  
Accepted 1 December 2018

### KEYWORDS

Epithelial ovarian cancer;  $\beta$ -hCG; invasion and metastasis; proliferation; ERK1/2

## 1. Introduction


Epithelial ovarian cancer (EOC) is the leading cause of mortality among gynecological malignancies [1,2]. Most EOC patients are asymptomatic, and, currently, there are no effective early screening methods; thus, the majority of patients are diagnosed at an advanced FIGO stage. Extensive pelvic and peritoneal spread is a key factor in the poor prognosis of advanced EOC [3–5]; however, the underlying mechanisms of EOC metastasis are still unclear.

Human chorionic gonadotropin (hCG), comprised of  $\alpha$ -subunit and  $\beta$ -subunit, refers to a group of 5 molecules that share a common amino acid sequence

but different oligomeric and carbohydrate side chain structures, including regular hCG, sulfated hCG (hCG-S), hyperglycosylated hCG (hCG-H), free  $\beta$ -subunit of hCG ( $\beta$ -hCG) and hyperglycosylated  $\beta$ -hCG ( $\beta$ -hCG-H) [6]. For functional roles, regular hCG molecule is produced by syncytiotrophoblast and indispensable for human pregnancy during embryo implantation, angiogenesis and development of the chorion, and hCG-S is produced by pituitary and related to the menstrual cycle [7]. The hCG-H is a structural variant of hCG produced by cytotrophoblast cells during gestational trophoblastic disease (GTD), invasive mole or choriocarcinoma [6]. The  $\beta$ -hCG and  $\beta$ -hCG-H, as autocrine growth factors, are

**CONTACT** Xiaoqing Guo  [Xiaoqing\\_Guo@tongji.edu.cn](mailto:Xiaoqing_Guo@tongji.edu.cn); Kai Wang  [kaiwangcn@yahoo.com](mailto:kaiwangcn@yahoo.com)

\*These authors contributed equally to this work.

 Supplemental data for this article can be accessed [here](#).

produced in most non-trophoblastic tumor cells, particularly gynecologic malignancies, including ovarian, endometrial and cervical cancers [8–10]. In our previous study,  $\beta$ -hCG was shown to promote proliferation and cell cycle progression, reduce apoptosis and facilitate tumor growth in normal ovarian surface epithelial cells [11]. In further study, we preliminarily demonstrated that  $\beta$ -hCG could aggressively increase EOC metastasis and invasion ability accompanied by EMT *in vitro* and *in vivo* [12].

In this study, histologically,  $\beta$ -hCG was significantly correlated with EOC metastasis, FIGO stage and other unfavorable clinicopathological features. In addition, a series of gain- and loss-of-function experiments revealed that  $\beta$ -hCG promotes EOC cells migration and invasion ability, invadopodia protrusion, mitochondria accumulation and cytoskeletal rearrangements *in vitro* and tumor metastasis in orthotopic ovarian cancer xenograft models *in vivo*. Moreover, ERK1/2 phosphorylation rescue experiments demonstrated that  $\beta$ -hCG facilitates EOC metastasis through activation of the  $\beta$ -hCG/ERK/MMP2 signaling pathway. This study is the first to demonstrate that  $\beta$ -hCG contributes to EOC dissemination through the ERK/MMP2 signaling pathway and thus may be a new target for therapeutic intervention.

## 2. Materials and methods

### 2.1. Patients and tissue samples

Studies involving humans were approved by the Ethical Committee of the First Affiliated Hospital of the Medical College of Shihezi University. Informed consent was obtained for studies involving human EOC and nonmalignant ovarian tissues. EOC patients diagnosed in the First Affiliated Hospital of the Medical College of Shihezi University between December 2006 to December 2013 were recruited from our previous study [12]. The available medical records, histologic slides, and paraffin-embedded tissue blocks associated with 10 cases of FIGO Stage I human nonmetastatic EOC and 24 cases of FIGO Stage II-IV primary and paired metastasis EOC tissues were included in this study, and 20 cases of nonmalignant ovarian tissues were used as controls. None of the patients had received prior adjuvant chemotherapy before surgery. All EOC samples

were pathologically diagnosed according to the World Health Organization (WHO) classification guidelines (2014).

### 2.2. Immunohistochemical staining

Immunohistochemistry (IHC) was performed as previously described [12]. Briefly, 4- $\mu$ m-thick tissue sections were stained with primary polyclonal antibodies against  $\beta$ -hCG (1:50; cat. ab53087, Abcam, USA), ERK (1:200; cat. 4695, Cell Signaling Technology, USA), p-ERK1/2 (1:200; cat. 4370, Cell Signaling Technology, USA), MMP-2 (1:100; cat. 10373-2-AP, Proteintech, USA) and Ki-67 (1:200; ab16667, Abcam, USA) diluted in antibody diluent (cat. 8112 L, Cell Signaling Technology, USA), then incubated with secondary antibody, and finally stained with 3,3-diaminobenzidine and hematoxylin.

### 2.3. ELISA

Equal volumes of serum samples were loaded into a plate precoated with mouse monoclonal anti- $\beta$ -hCG antibody (R&D Systems, MN, USA) and incubated with HRP-conjugated monoclonal anti- $\beta$ -hCG detection antibody at 37°C for 1 h. After a brief wash, substrate solution was added and incubated in the wells for 15 min. The reaction was stopped by application of Stop Solution. The colorimetric signals were measured using a microplate reader (BioRad, CA, USA). A standard curve with known amounts of recombinant human  $\beta$ -hCG was also constructed to calculate the absolute quantity of  $\beta$ -hCG present in each sample. The  $\beta$ -hCG value was normalized to the total protein content of each sample, as measured by the Bradford method.

### 2.4. Cell culture and construction of $\beta$ -hCG dysregulated EOC cells

The human EOC cell lines ES-2, OVCAR-3 and SKOV3 obtained from the Shanghai Cell Bank of Chinese Academy of Sciences were cultured in RPMI-1640 medium (HyClone) containing 10% fetal bovine serum (FBS, Gibco), 100 units/mL penicillin, and 100 mg/mL streptomycin at 37°C in a humidified 5% CO<sub>2</sub> incubator. Upon resuscitation, the cell lines were characterized by Genetic Testing Biotechnology Corporation (Suzhou, China) using

short tandem repeat (STR) markers (Supplemental file S1). The  $\beta$ -hCG up-/downregulation EOC cell models were constructed as previously described [12]. Briefly, ES-2 and OVCAR-3 cells were stably transduced with lentiviral vector encoding  $\beta$ -hCG (LV- $\beta$ -hCG) or negative control (LV-vector), while SKOV3 cells were transiently transfected with  $\beta$ -hCG-siRNAs or nc-siRNA. Then, the efficiency of  $\beta$ -hCG dysregulation was assessed using qPCR and western blotting assays.

### 2.5. Cell viability assay

Cell proliferation was determined using Cell Counting Kit-8 (CCK-8, cat. KGA317, KeyGen BioTECH, China) according to the manufacturer's instructions. Briefly,  $2.0 \times 10^4$  ovarian cancer cells were seeded in 96-well plates with 100  $\mu$ l of maintenance medium. The number of viable cells after two hours of incubation was assessed by measurement of the absorbance at 450 nm using a microplate reader (BioTek Instruments, Winooski, VT, USA). The viability rate was calculated as the experimental OD value/control OD value.

### 2.6. Colony-formation assay

For colony-formation assays, cells were plated on 6-well plates at a concentration of 150 cells/well and incubated for approximately 2 weeks. Then, cell colonies were observed, fixed with 100% methanol and stained with hematoxylin.

### 2.7. Cell cycle analysis with flow cytometry (FCM)

ES-2, OVCAR-3 and SKOV3 cells were collected after trypsin digestion and fixed with 70% ethanol overnight at 4°C. After fixation, the cells were washed with PBS two times and treated with RNaseA and propidium iodide (PI, 50  $\mu$ g/ml) for 30 min. Then, a FACScalibur flow cytometer (BD Biosciences, USA) with FACSDiva software (BD Bioscience, USA) was used to analyze the cell cycle distribution, and the data were modified using ModFit LT 3.2 software (Verity Software House, USA).

### 2.8. Cell migration and invasion assays

For cell migration and invasion assays,  $1.0 \times 10^5$  cells in 150  $\mu$ L RPMI-1640 with 2% FBS were cultured in the upper chambers of 8- $\mu$ m transwell inserts (Corning, cat. 351158) with Matrigel (invasion) or without Matrigel (migration) in a 24-well plate. After 16–48 h of incubation, the cells remaining in the upper side of the inserts were gently removed. Tumor cells attached to the lower surface of the membrane were stained with calcein AM (0.625  $\mu$ g/ml; cat.1537419, Thermo Fisher Scientific, USA) or hematoxylin. Migrated cells were photographed at 100  $\times$  magnification under a fluorescence microscope or an inverted microscope, and the number of migratory/invasive cells was calculated in five randomly selected fields.

### 2.9. Electron microscopy

For Scanning Electron Microscope (SEM) preparations,  $1.0 \times 10^5$  ES-2 and SKOV3 cells were seeded on coverslips precoated with Matrigel matrix. The cells were fixed with 2.5% glutaraldehyde in 0.1 M cacodylate buffer (pH 7.3) with 2% sucrose at room temperature for 20 min and then dehydrated through a graded ethanol series, critical point-dried in CO<sub>2</sub>, and gold coated via sputtering. The samples were then examined using a Hitachi S-4800 scanning electron microscope (Hitachi).

For Transmission Electron Microscope (TEM) preparations,  $1.0 \times 10^7$  ES-2 and SKOV3 cells were fixed with 2.5% glutaraldehyde in 0.1 M sodium cacodylate buffer (pH 7.4) at 4°C overnight and then postfixed with 1% OsO<sub>4</sub> solution in 0.1 M sodium cacodylate buffer (pH 7.4) at 4°C for 1.5 h. After dehydration in an ethanol gradient (50–100%, 15 min each), samples were embedded in EPON812 at 60°C for 2 days. Ultrathin sections (70 nm) were obtained, placed on copper grids and stained using uranyl acetate and lead citrate. Observations were carried out with an FEI Tecnai G2 spirit TEM (FEI), and images were acquired using an Olympus X71 microscope (Tokyo).

### 2.10. Immunofluorescence staining

For immunofluorescence staining, the cells were fixed with methanol and incubated with primary

antibody against cortactin (cat. ab81208, Abcam), followed by incubation with Alexa 488-conjugated secondary antibody (Sigma). Fluorescent staining for cortactin was visualized via confocal laser-scanning microscopy (TCS SP5, Leica), using TRITC-conjugated phalloidin (cat. P1951, Sigma) and DAPI to counterstain F-actin and the nuclei, respectively.

### **2.11. Construction of subcutaneous and orthotopic ovarian xenograft tumor models in nude mice**

All animal experiments were approved by the Institutional Use and Care of Animals Committee and conducted according to the approved animal protocol of the Animal Centre of Tongji University. Animal experiments were performed according to the institutional guidelines and animal research principles. Female nude mice, aged 4 to 6 weeks (weighing approximately 20 g), were housed and cared for at the Animal Centre of Tongji University (Shanghai, China).

For subcutaneous ovarian xenografts,  $1 \times 10^6$  ES-2 and OVCAR-3 cells transduced with LV- $\beta$ -hCG or LV-vector in 100  $\mu$ l PBS were subcutaneously injected into the left and right flanks of mice, respectively. Tumor length (L) and width (W) were measured every 3 days using a digital Vernier caliper. Tumor volume was determined using the following formula: volume =  $L \times W^2 / 2$ . Mice were sacrificed according to tumor burden, and xenografts were excised and weighed.

For orthotopic ovarian xenografts [13], nude mice were anaesthetized with isoflurane, the skin was disinfected with Betadine, and the left ovary and oviduct were exteriorized through a 1- to 2-cm lateral midline skin incision on the back. Then,  $5 \times 10^5$   $\beta$ -hCG-overexpressing ES-2 and OVCAR-3 cells and control cells were resuspended in 10  $\mu$ l PBS and injected under the ovarian bursa of the mice using a 32-gauge syringe (cat. 80386, Hamilton). After injection, the ovaries were replaced in the peritoneal cavity, and the peritoneal cavity and skin were sequentially closed and disinfected. Xenograft growth was monitored with a NightOWL LB 983 *In Vivo* Imaging System (Berthold Technologies) every two days. Mice were sacrificed 40 days after inoculation of the

orthotopic ovarian xenografts or according to tumor burden. After that, tumor grafts and peritoneal nodules were fixed in 10% formalin and subjected to routine histological examination and IHC staining. Furthermore, the  $\beta$ -hCG, ERK, p-ERK1/2, MMP-2 and Ki-67 protein expression in xenografts was assessed by western blotting.

### **2.12. Inhibition of the ERK1/2 signaling pathway**

ES-2 and SKOV3 cells were incubated with the specific ERK1/2 phosphorylation inhibitor SCH772984 (2 mM; cat. S7101, Selleck, USA) in 1% serum medium for 24 hours. Control cells were treated with the same volume of dimethyl sulfoxide (DMSO). After incubation, the efficacy of ERK pathway inhibition was detected by western blotting.

### **2.13. Quantitative RT-PCR (qRT-PCR)**

qRT-PCR analysis was performed as previously described [12]. Briefly, total RNA was extracted with Trizol Reagent (Invitrogen), and cDNA was synthesized using a reverse transcription kit (TaKaRa). The  $\beta$ -hCG mRNA level was measured using a Super Real PreMix Plus (SYBR Green) Kit (KeyGen BioTECH) and an Applied Biosystems Step One Plus<sup>TM</sup> Real-Time PCR System. The relative  $\beta$ -hCG mRNA level was calculated using the  $2^{-\Delta\Delta C_t}$  method, and GAPDH was used as the positive control. The qRT-PCR primers were as follows:

GAPDH, (forward) 5'-ACAACCTTTGGTATCGT GGAAGG-3'

and (reverse) 5'-GCCATCACGCCACAGTTTC-3';

$\beta$ -hCG, (forward) 5'-TCTGTGCCGGCTACTGCC CC-3'

and (reverse) 5'-TTGGGACCCCCGCAGTCA GT-3'.

### **2.14. Western blot analysis**

Total protein from cells and tissues was lysed in Whole Cell Lysis Assay buffer (cat. KGP250, KeyGen BioTECH, China) containing protease inhibitors (cat. KGP603, KeyGen BioTECH, China) and phosphatase inhibitors (cat. KGP602, KeyGen BioTECH, China). Then, 30  $\mu$ g of protein per sample was resolved on 10% SDS-PAGE gels and transferred

onto PVDF membranes. The membranes were first incubated overnight at 4°C in TBS containing BSA, 0.05% Tween 20, and primary antibodies against GAPDH (1:4000; cat. M20006S, Abmart, USA),  $\beta$ -hCG (1:1000; cat. AP13036b, Abgent, USA), luteinizing hormone/chorionic gonadotropin receptor (LHCGR) (1:1000, cat. 19968-1-AP, Proteintech, USA), ERK1/2 (1:1000; cat. 4695, Cell Signaling Technology, USA), P-ERK1/2 (1:1000; cat. 4370, Cell Signaling Technology, USA) and MMP-2 (1:1000; cat. 10373-2-AP, Proteintech, USA), followed by incubation with secondary antibodies (cat. KGAA3d5, KeyGen BioTECH, China) conjugated with horseradish peroxidase at room temperature for 1 h. The protein bands were detected using an enhanced chemiluminescence plus kit (Millipore) according to the manufacturer's recommendations.

### 2.15. Statistical analysis

All experiments were repeated at least three times in duplicate. Data are presented as the mean  $\pm$  SD. Differences between the treated and control groups were analyzed using Student's t-test, and the associations between various demographic parameters were evaluated by Fisher's exact test. The level of significance was set at  $P < 0.05$ . All statistical analyzes were performed with GraphPad Prism 7.0 software (GraphPad Software, USA).

## 3. Results

### 3.1. $\beta$ -hCG expression is strongly associated with unfavourable clinical features in EOC

All the tumor samples collected in this study, involved 26 cases of ovarian serous carcinoma, 6 cases of ovarian mucinous carcinoma, and 2 case of ovarian endometrial carcinoma, and the metastatic samples were primarily from the omentum and mesenterium in FIGO stage II-IV cases. The IHC results showed that the positive rate of  $\beta$ -hCG was gradually elevated in nonmalignant ovarian (5%), FIGO stage I (30%) and II-IV primary EOC tissues (54.2%), with the highest  $\beta$ -hCG expression in paired metastatic EOC tissues (83.3%) ( $P < 0.05$ ) (Supplemental Figure S1 A,B). In addition,  $\beta$ -hCG positivity is strongly associated with unfavorable clinical features of EOC,

especially with FIGO Stage III-IV EOC,  $>5$  cm tumor size, poor differentiation, Type II histological grade and high grade serous ovarian carcinoma (HGSOC) ( $P < 0.05$ ), compared with FIGO Stage I EOC,  $\leq 5$  cm tumor size, well or moderate differentiation, Type I histological grade and low grade serous ovarian carcinoma (LGSOC), respectively (Table 1). However, serological  $\beta$ -hCG expression was not significantly different between EOC and nonmalignant ovarian patients ( $P > 0.05$ ) (Supplemental Figure S1 C).

### 3.2. $\beta$ -hCG dysregulated EOC cell models were successfully constructed

$\beta$ -hCG expression was evaluated in three parental EOC cell lines: ES-2, OVCAR-3 and SKOV3. As the results show,  $\beta$ -hCG mRNA and protein levels were the highest in SKOV3 cells compared with ES-2 and OVCAR-3 cells (Figure 1(a)). Next, to elucidate the biological functions of  $\beta$ -hCG in EOC, dysregulated  $\beta$ -hCG EOC cell models were constructed. As the results show, OVCAR-3 cells with stable  $\beta$ -hCG upregulation were successfully constructed (Figure 1(b,c)) ( $P < 0.05$ ). Additionally, the ES-2 cells with  $\beta$ -hCG upregulation and SKOV3 cells with  $\beta$ -hCG downregulation had been constructed in our previous research [12].

### 3.3. $\beta$ -hCG showed no dramatic effects in regulating EOC proliferation in vitro and in vivo

To investigate the effects of  $\beta$ -hCG on tumor proliferation, *in vitro* CCK-8, colony-formation, and FCM cell cycle analysis assays and *in vivo* nude mouse subcutaneous xenograft assays were performed. As the results show, colony formation and cell viability were not significantly regulated by  $\beta$ -hCG (Figure 2(a,b)). In addition, the FCM results showed no obvious differences in cell cycle distribution between dysregulated  $\beta$ -hCG cells and the control cells (Figure 2(c)). Furthermore, upregulation of  $\beta$ -hCG was found to have no significant effects on tumor volume or the weight of subcutaneous xenografts in nude mice (Figure 2(d)), even with positive Ki-67 expression in xenograft tissues based on IHC (Figure 2(e)).

**Table 1.** Correlation between  $\beta$ -hCG expression level and patient clinicopathological features.

Clinicopathological parameters	Number of cases	Tissue $\beta$ -hCG (N = 34)		
		Positive	$\chi^2$	P value
Age (years)				
$\leq 60$	15	7	2.542	0.110
$> 60$	19	15		
FIGO stage				
I	10	3	8.931	<b>0.011</b>
II	8	5		
III-IV	16	14		
Tumor size (cm)				
$\leq 5$	10	3	5.474	<b>0.019</b>
$> 5$	24	19		
Differentiation				
Well or moderate	12	4	6.010	<b>0.014</b>
Poorly	22	18		
Histological grade				
Type I	12	7	4.30	<b>0.038</b>
Type II	22	6		
Lymphnode metastasis				
Positive	16	5	0.350	0.055
Negative	18	3		
Serum CA-125 level (U/ml)				
$\geq 35$	34	24	/	/
$< 35$	0	0		
Histological pathology				
Serous	26	19	0.530	0.767
Mucinous	6	4		
Endometrial	2	1		
Ovarian serous carcinoma subtypes				
Low grade serious ovarian carcinoma	6	2	3.91	<b>0.047</b>
High grade serious ovarian carcinoma	20	17		

### 3.4. $\beta$ -hCG significantly regulated migration, invasion and ultrastructure of EOC cells in vitro

Migration and invasion transwell assay results revealed that upregulation of  $\beta$ -hCG greatly increased the number of ES-2 and OVCAR-3 cells that penetrated the membrane ( $P < 0.001$ ), while downregulation of  $\beta$ -hCG dramatically decreased that of SKOV3 cells ( $P < 0.001$ ) (Figure 3(a,b)).

Next, remarkably longer and more extended invadopodia protrusions were found on the surface of  $\beta$ -hCG-overexpressing ES-2 cells under SEM, with more mitochondria assembled around invadopodia observed under TEM (Figure 3(c)), while fewer and stunted invadopodia were observed with  $\beta$ -hCG downregulation in SKOV3 cells, with less mitochondria gathered on the cell surface compared with control cells (Figure 3(d)).

Furthermore, the cytoskeletal markers F-actin and cortactin were significantly induced by upregulation of  $\beta$ -hCG in ES-2 cells based on immunofluorescence staining observed under a confocal microscope (Figure 3(e)), while SKOV3 cells with

$\beta$ -hCG downregulation showed the opposite effects, suggesting that the cytoskeleton of EOC cells is remarkably mediated by  $\beta$ -hCG.

### 3.5. $\beta$ -hCG greatly facilitates EOC metastasis and dissemination in nude mouse orthotopic ovarian tumor models

To construct nude mouse orthotopic ovarian tumor models,  $\beta$ -hCG-overexpressing ES-2 and OVCAR-3 cells were intrabursally injected into the ovaries of nude mice. As the results show, the metastasis and dissemination of xenografts were significantly promoted by  $\beta$ -hCG, as detected with a NightOWL LB 983 *In Vivo* Imaging System (Figure 4(a)). After dissection, the nodular lesions were confirmed to be EOC tissues by pathology experts via H&E staining, and  $\beta$ -hCG was remarkably upregulated in the corresponding groups by IHC staining (Figure 4(b)). Moreover, gross visualization showed that a more severe tumor burden and more metastatic nodule lesions in the omentum, mesentery, peritoneum and

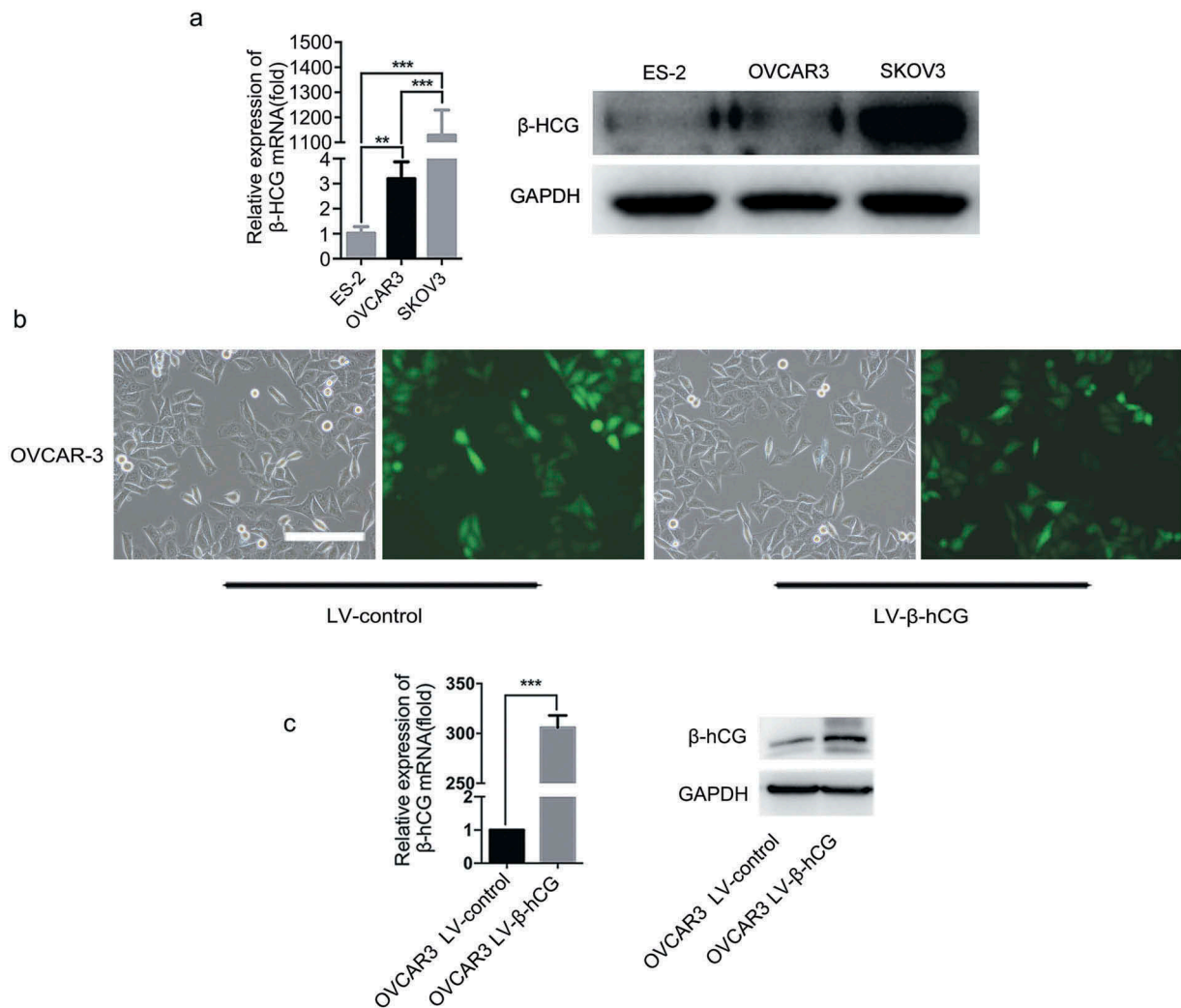


**Figure 1.** Expression of  $\beta$ -hCG in EOC cell lines. (a) The mRNA and protein expression of  $\beta$ -hCG in EOC cell lines was examined by RT-PCR and western blot analysis. (b and c). Successful construction of  $\beta$ -hCG-overexpressing OVCAR-3 cells. The relative expression level of  $\beta$ -hCG mRNA and protein were determined by RT-PCR analysis and western blotting. Scale bar, 100  $\mu$ m, \*\* $P < 0.01$ , \*\*\* $P < 0.001$ .

diaphragm were induced by  $\beta$ -hCG compared with control groups. Furthermore, the number and weight of metastatic nodules (diameter  $> 2$  mm) were also remarkably enhanced by  $\beta$ -hCG (Figure 4(c)).

### 3.6. $\beta$ -hCG promotes EOC metastasis through the ERK/MMP2 pathway *in vitro*

To further elucidate the mechanisms involved in the tumor dissemination mediated by  $\beta$ -hCG in EOC, a series of experiments were carried out. First, the phosphorylation level of ERK1/2 and the expression of MMP2 were found to be positively correlated with  $\beta$ -hCG in primary EOC and paired metastatic EOC

tissues by IHC staining (Figure 5(a)). Next, the phosphorylation level of ERK1/2 and the expression of MMP2 were upregulated in  $\beta$ -hCG-overexpressing ES-2 and OVCAR3 cells, while knockdown of  $\beta$ -hCG in SKOV3 cells caused the opposite effects *in vitro* (Figure 5(b)). In addition, consistent with the *in vitro* experiments, the phosphorylation level of ERK1/2 and MMP2 expression was significantly increased in  $\beta$ -hCG-overexpressing xenografts based on western blot analysis and IHC compared with the control group (Figure 5(c,d)). The above results suggest that the ERK1/2 pathway may be involved in the tumor metastasis induced by  $\beta$ -hCG.

To further explore the involvement and function of ERK1/2 activation in metastasis induced by

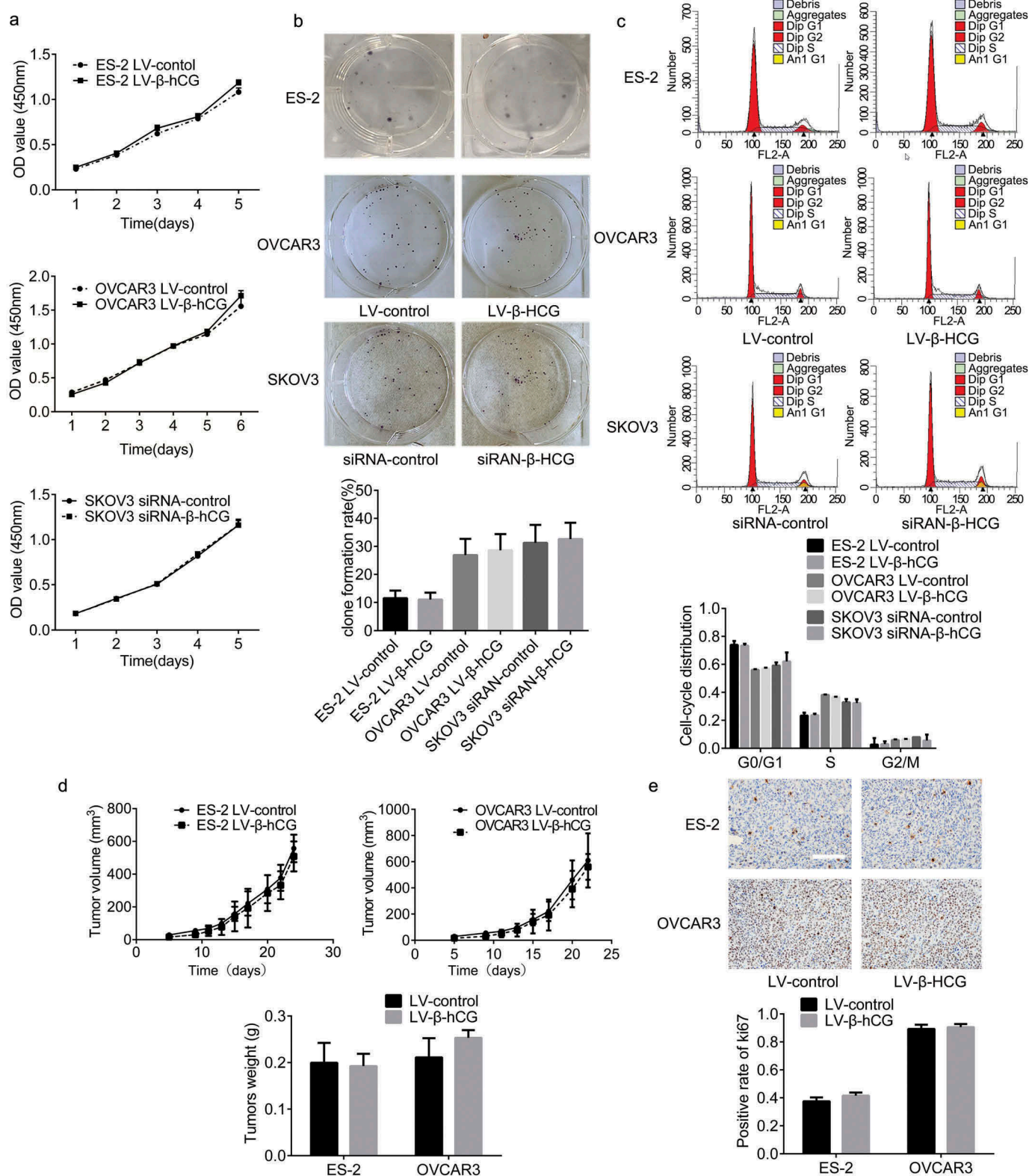


**Figure 2.**  $\beta$ -hCG had no significant influence on EOC cell proliferation *in vitro* or *in vivo*. (a and b) The effect of  $\beta$ -hCG on ES-2 and SKOV3 cell proliferation was detected by CCK8 analysis and colony formation assays. (c) The effect of  $\beta$ -hCG on cell cycle was assessed using FCM. (d) The tumor growth curve of subcutaneous ovarian xenografts was continuously detected with a digital Vernier caliper. The tumor weights in each group were quantified. (e) Representative immunohistochemical staining of Ki-67 in xenograft tumor tissues. Scale bar, 50  $\mu$ m.



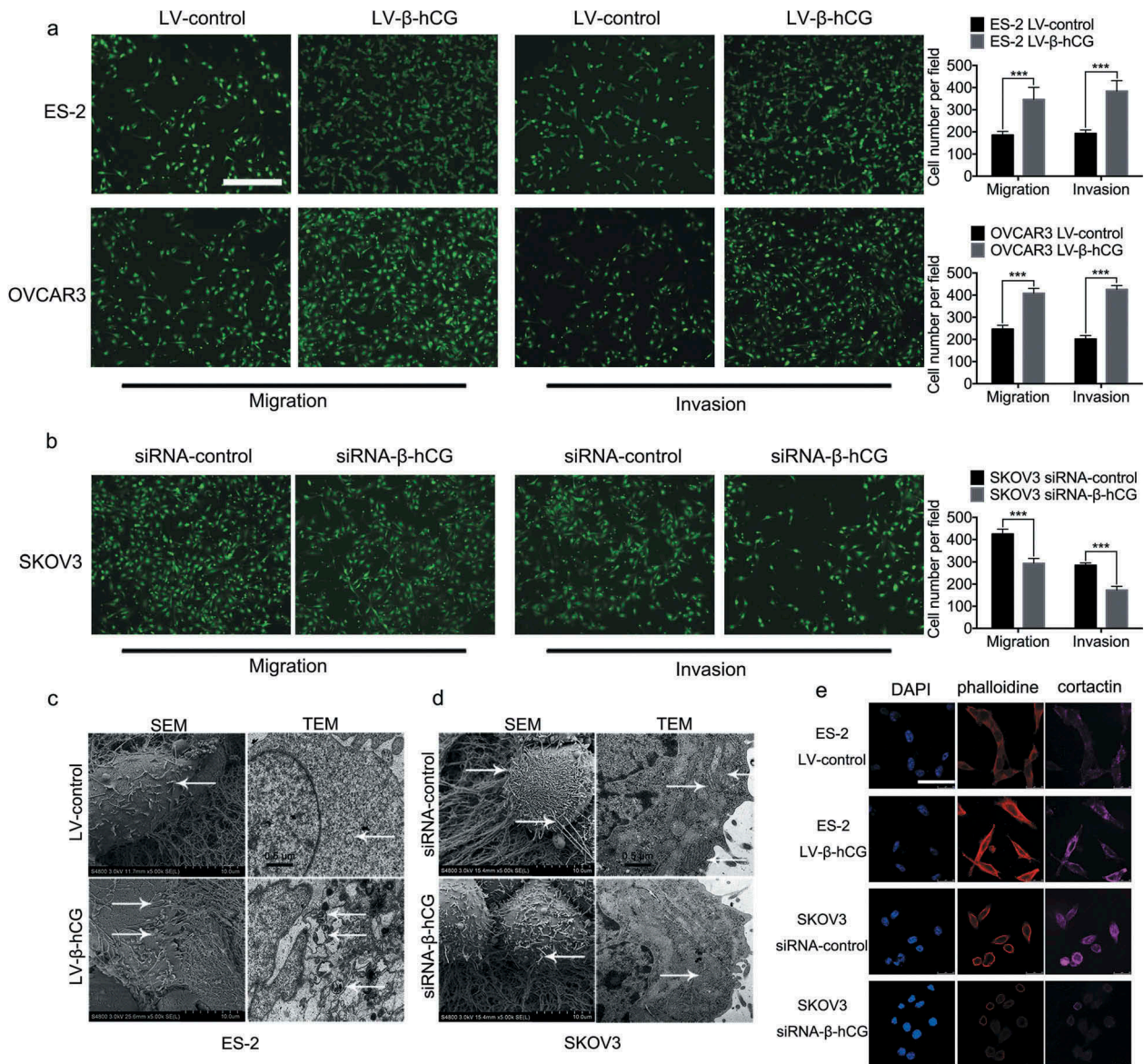


**Figure 3.** Transwell assays and ultrastructural changes were found in  $\beta$ -hCG dysregulated EOC cells *in vitro*. (a and b) Transwell assays showed that  $\beta$ -hCG regulates EOC cell migration and invasion *in vitro*. Scale bar, 200  $\mu$ m, \*\*\* $P$  < 0.001. (c and d) SEM and TEM showed increased invadopodia and chondriosomes (white arrows) in  $\beta$ -hCG-overexpressing ES-2 cells and SKOV3 cells with  $\beta$ -hCG downregulated. (e) Immunofluorescence staining of cortactin and F-actin in dysregulated EOC cells. Scale bar, 50  $\mu$ m.

$\beta$ -hCG in EOC, ERK phosphorylation rescue experiments were implemented. As the results show, the specific ERK1/2 phosphorylation inhibitor SCH772984 significantly reduced the migration and invasion ability of parental SKOV3 and  $\beta$ -hCG-overexpressing ES-2 cells (Figure 5(e)). In addition, western blot analysis showed that p-ERK1/2 and MMP2, which were originally upregulated after  $\beta$ -hCG overexpression, were obviously decreased. Moreover, this effect did not influence the  $\beta$ -hCG expression level (Figure 5(f)).

#### 4. Discussion

$\beta$ -hCG is well-known as a sensitive biomarker for trophoblastic tumors and diseases. Recently, studies have found that  $\beta$ -hCG was ectopically elevated in the histological and serological samples of renal cell carcinoma [14], hepatocellular carcinoma [15], gastric cancer [16] and colon cancer patients [17]. Moreover,  $\beta$ -hCG was regarded as a biomarker to surveil recurrence and follow-up of malignant germ cell and sex cord-stromal tumors as Class 2B evidence in the 2018 NCCN clinical practice guidelines in Ovarian Cancer

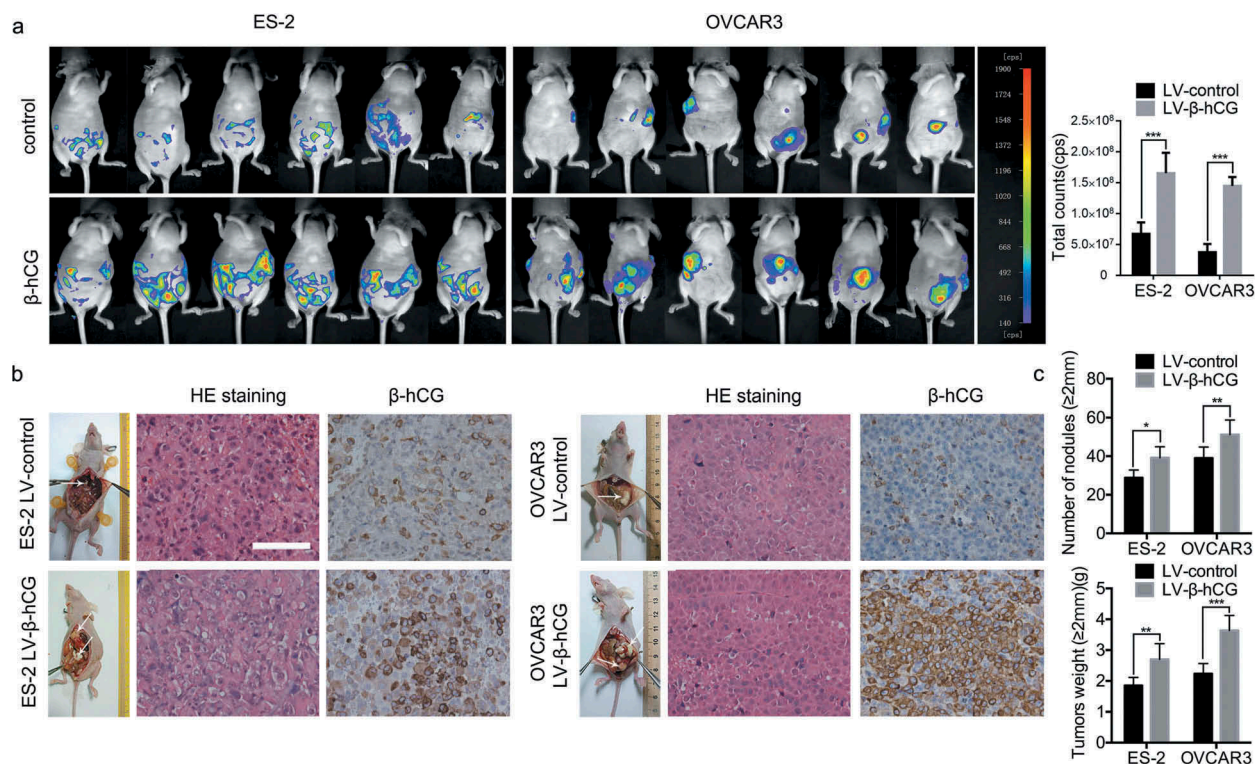


**Figure 4.**  $\beta$ -hCG enhanced cancer cell metastasis in an orthotopic ovarian xenograft tumor model. (a) The growth of orthotopic ovarian xenografts was detected with a NightOWL LB 983 In Vivo Imaging System. (b) After sacrifice, the ovarian tumors in nude mice were removed and are shown by white arrows in the images. Representative pictures of H&E staining and  $\beta$ -hCG immunohistochemical staining of nodular lesions. Scale bar, 50  $\mu$ m. (c) The average number of peritoneal tumor nodules and average weight of tumors from each group were quantified. \* $P < 0.05$ , \*\* $P < 0.01$ , \*\*\* $P < 0.001$ .

[18]. In our previous study,  $\beta$ -hCG was verified to promote the malignant transformation of human ovarian epithelial cells, additionally its immunoreactivity was remarkably elevated in malignant ovarian tissues, compared with normal ovaries tissues [11,12]. In this study, aberrant  $\beta$ -hCG expression was found to be remarkably associated with unfavorable clinicopathological features of EOC, including FIGO stage, tumor size, differentiation, histologic grade and HGSOC, especially the highest expression in metastatic tissues, which suggested that elevated histological  $\beta$ -hCG expression can be used to evaluate the severity and progression of EOC. Therefore, the roles and mechanisms of  $\beta$ -hCG in EOC tumorigenesis and metastasis was worth to be further explored.

Whether  $\beta$ -hCG plays a vital role in regulating tumor proliferation is still controversial. Some scholars have verified that  $\beta$ -hCG dramatically promotes proliferation in nontrophoblastic solid tumors, such as bladder carcinoma, pituitary adenoma, choriocarcinoma and endometrial cancer

[19–21]. In contrast, some scholars have found that  $\beta$ -hCG significantly suppresses breast cancer cell viability *in vitro* and inhibits tumor growth and attenuates tumor vessel formation *in vivo* [22]. In addition,  $\beta$ -hCG was confirmed to have no effect on the proliferation of colorectal cancer cells [23]. In this study,  $\beta$ -hCG was validated to have no significant influence on the proliferation of EOC *in vitro* and *in vivo*.

Previous studies have demonstrated that tumor cells ultrastructural abnormalities, including invadopodia protrusions, mitochondria aggregation and cytoskeletal rearrangement, are closely related to more aggressive phenotype with greater migration and invasion ability [24–26], in which actin cytoskeleton regulators, including cortactin, F-actin, N-WASp and Arp2/3 were abnormally enriched [27–29]. In our study, immunofluorescence staining of cortactin and F-actin showed that upregulation of  $\beta$ -hCG significantly induced invadopodia protrusion and cytoskeleton

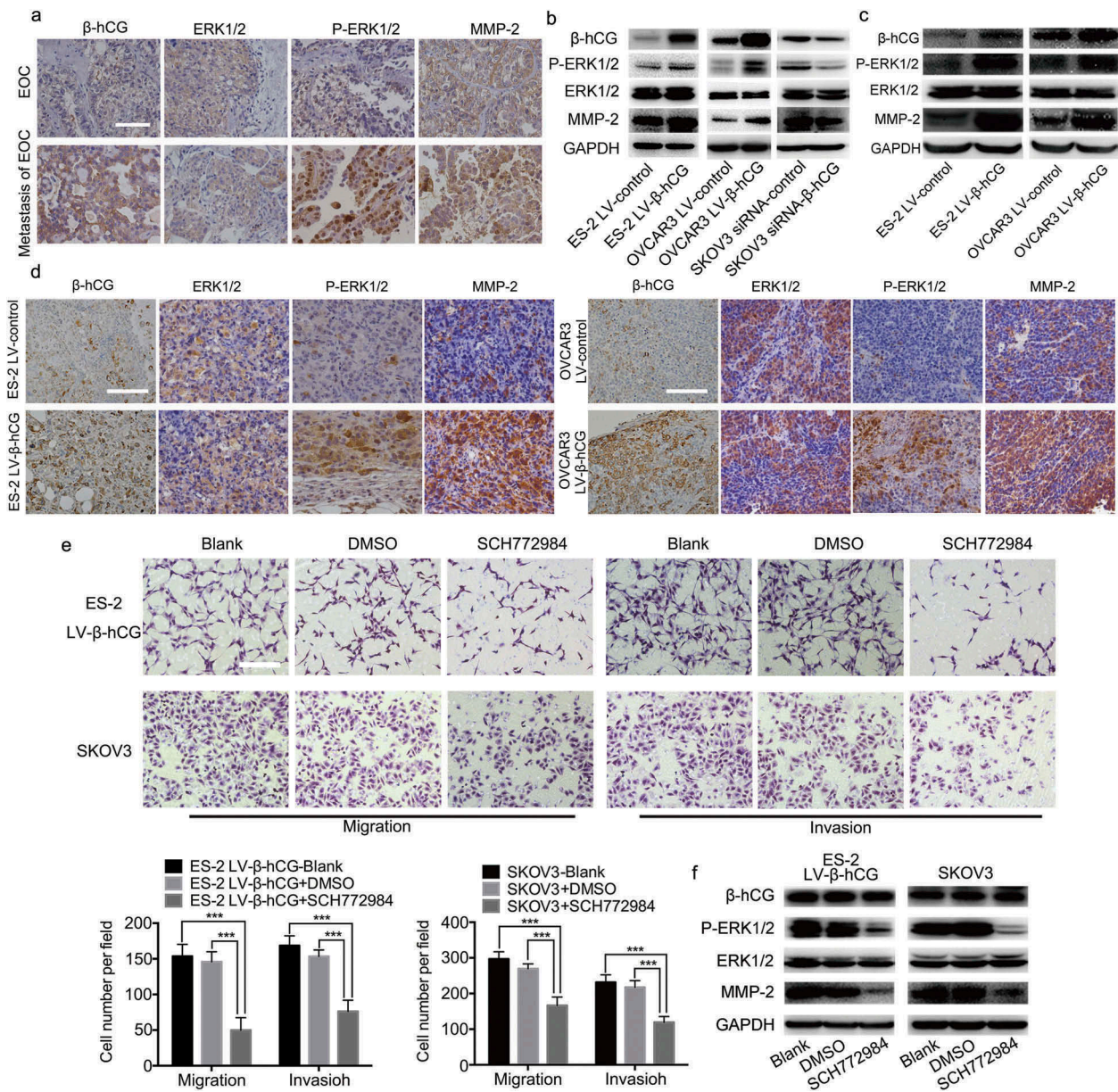


**Figure 5.**  $\beta$ -hCG enhanced EOC cell migration and invasion via the ERK1/2 signaling pathway *in vitro*. (a) Representative images of  $\beta$ -hCG, ERK1/2, p-ERK1/2 and MMP2 immunohistochemical staining of surgical specimens from primary and metastatic EOC tissue. Scale bar, 50  $\mu$ m. (b) The expression of  $\beta$ -hCG, ERK1/2, p-ERK1/2 and MMP2 protein in EOC cells was detected by western blot. (c and d) The expression of  $\beta$ -hCG, ERK1/2, p-ERK1/2 and MMP2 in orthotopic ovarian xenografts was determined by western blot and IHC. Scale bar, 50  $\mu$ m. (e). The ERK1/2-specific inhibitor SCH772984 (2 mM) suppressed the migratory and invasive ability in  $\beta$ -hCG-overexpressing ES-2 and SKOV3 cells. Scale bar, 200  $\mu$ m, \*\*\* $P$  < 0.001. (f). The p-ERK1/2 and MMP2 protein expression in  $\beta$ -hCG-overexpressing ES-2 and SKOV3 cells rescued by SCH772984 was determined via western blot analysis.

rearrangement. Mitochondria are the major source of cellular ATP and are essential for maintaining cell biological activities, including cell growth, division and movement [30,31], and increased accumulation of mitochondria can dramatically promote invadopodia extension and tumor metastasis in breast cancer and colon cancer [32,33]. In this study, more mitochondria were found

gathered on the edge of invadopodia in  $\beta$ -hCG-overexpressing cells. These results strongly suggest that the metastatic phenotype of EOC cells was strongly facilitated by  $\beta$ -hCG.

The tumor microenvironment plays a vital role in tumorigenesis and progression, and estrogenic hormone was confirmed to be closely related to EOC [1]. Due to its simple construction method

and ease of observation, the subcutaneous xenograft animal model is frequently used to mimic the tumor proliferation microenvironment, and  $\beta$ -hCG was shown to have little effect on EOC proliferation in this study. The orthotopic ovarian xenograft model can maximally recapitulate the microenvironment and biological behavior of human EOC, thus it is often utilized as an optimal animal model for simulating tumor progression [34,35]. In this study, orthotopic ovarian xenograft tumor models were constructed to verify the roles and mechanisms of  $\beta$ -hCG in regulating EOC tumor metastasis. As the results show, the xenografts were confirmed to be ovarian adenocarcinoma by pathology experts, and the widespread pelvic and peritoneal metastases were extremely similar to those observed in human EOC, importantly more severe tumor burden was observed in  $\beta$ -hCG-overexpressing groups.

The ERK/MMP-2 signaling pathway is one of the key triggers of metastasis in human cancer [36,37]. When stimulated, ERK is converted to phosphorylated ERK; then, AP-1 and the promoter of ERK downstream target MMPs are activated and translated. Consequently, the extracellular matrix (ECM) is abnormally degraded, and the necessary extracellular microenvironment for tumor cell metastasis is gradually provided [38–42]. In this study, we confirmed that p-ERK1/2 rather than ERK1/2 was strongly regulated by  $\beta$ -hCG in EOC cell lines, orthotopic ovarian xenograft and human EOC tissues. Moreover, the increased invasion ability of EOC cells induced by  $\beta$ -hCG could be reversed by the specific p-ERK1/2 inhibitor SCH772984 *in vitro*.

It is well-known that hCG represents a key embryonic signal which is essential for pregnancy; as a structural homogeneity of luteinizing hormone (LH), it is primarily linked to the LHCGR to achieve corresponding functions [43]. Activated LHCGR can stimulate adenylate cyclase, phospholipase C and ion channels which, in turn, control levels of intracellular cAMP, and promote cytotrophoblast fusion and microvilli formation with both actions essential for protein secretion and nutrient/gas exchange by the resulting syncytiotrophoblasts [43,44]. However, the regulation mechanisms of hCG on tumorigenesis was not always directly achieved by binding to LHCGR [45,46]. Researches have validated that LHCGR was negatively related to EOC, poor-

differentiated phenotype and unfavorable prognosis, meanwhile representative EOC cell line SKOV3 was proven to not express this receptor [47]. In addition, studies demonstrated that  $\beta$ -hCG may regulate EOC apoptosis suppression through an LHCGR-independent mechanism [48,49]. In this study, the LHCGR expression was confirmed to have no significant correlation with  $\beta$ -hCG expression in EOC cells and tissues (Supplemental figure S2), which indicated that the effects of  $\beta$ -hCG on EOC metastasis and invasion were LHCGR-independent.

In summary, our data show that  $\beta$ -hCG expression in human EOC is associated with unfavorable clinicopathological features. Although  $\beta$ -hCG was proved to have no significant effects on EOC cell proliferation or tumor growth, we found that the metastatic ability and phenotype of EOC cells was dramatically modulated by  $\beta$ -hCG *in vitro* and *in vivo*. Moreover,  $\beta$ -hCG-promoted metastasis was remarkably counteracted by a specific p-ERK1/2 inhibitor *in vitro*. Taken together, these data not only confirm the contribution of  $\beta$ -hCG to EOC metastasis, but also illuminate the novel mechanisms of the  $\beta$ -hCG/ERK/MMP2 signaling pathway in EOC metastasis.

## Acknowledgments

Xiaoqing Guo and Kai Wang conceived and designed the experiments; Weimin Wu, Hao Gao, Xiaofeng Li, Na Liu Shumin Peng and Guangxi Zhan performed the experiments; Jing Yu analyzed the pathological results; Xiaofeng Li analyzed the data; Weimin Wu and Na Liu wrote the paper. All authors read and approved the final manuscript.

## Funding

This work was supported by National Natural Science Foundation of China (grant number 8137230), Shanghai Municipal Medical and Health Discipline Construction Project (grant number 2017ZZ02015), and the Fundamental Research Funds for the Central Universities (grant numbers 22120170047 and 22120170104).

## References

- [1] Jayson GC, Kohn EC, Kitchener HC, et al. Ovarian cancer. *Lancet*. 2014;384:1376–1388.
- [2] May T, Yang J, Shoni M, et al. BRCA1 expression is epigenetically repressed in sporadic ovarian cancer cells

- by overexpression of C-terminal binding protein 2. *Neoplasia*. 2013;15:600–608.
- [3] Naora H, Montell DJ. Ovarian cancer metastasis: integrating insights from disparate model organisms. *Nat Rev Cancer*. 2005;5:355–366.
- [4] Bast RC Jr., Hennessy B, Mills GB. The biology of ovarian cancer: new opportunities for translation. *Nat Rev Cancer*. 2009;9:415–428.
- [5] Yeung TL, Leung CS, Yip KP, et al. Cellular and molecular processes in ovarian cancer metastasis. A review in the theme: cell and molecular processes in cancer metastasis. *Am J Physiol Cell Physiol*. 2015;309:C444–56.
- [6] Cole LA. HCG variants, the growth factors which drive human malignancies. *Am J Cancer Res*. 2012;2:22–35.
- [7] Prast J, Saleh L, Husslein H, et al. Human chorionic gonadotropin stimulates trophoblast invasion through extracellularly regulated kinase and AKT signaling. *Endocrinology*. 2008;149:979–987.
- [8] Muller CY, Cole LA. The quagmire of hCG and hCG testing in gynecologic oncology. *Gynecol Oncol*. 2009;112:663–672.
- [9] Cole LA. hCG, five independent molecules. *Clin Chim Acta*. 2012;413:48–65.
- [10] Gao S, Fan C, Huang H, et al. Effects of HCG on human epithelial ovarian cancer vasculogenic mimicry formation in vivo. *Oncol Lett*. 2016;12:459–466.
- [11] Guo X, Liu G, Schauer IG, et al. Overexpression of the beta subunit of human chorionic gonadotropin promotes the transformation of human ovarian epithelial cells and ovarian tumorigenesis. *Am J Pathol*. 2011;179:1385–1393.
- [12] Liu N, Peng SM, Zhan GX, et al. Human chorionic gonadotropin beta regulates epithelial-mesenchymal transition and metastasis in human ovarian cancer. *Oncol Rep*. 2017;38:1464–1472.
- [13] Yakubov B, Chelladurai B, Schmitt J, et al. Extracellular tissue transglutaminase activates noncanonical NF-kappaB signaling and promotes metastasis in ovarian cancer. *Neoplasia*. 2013;15:609–619.
- [14] Hotakainen K, Ljungberg B, Haglund C, et al. Expression of the free beta-subunit of human chorionic gonadotropin in renal cell carcinoma: prognostic study on tissue and serum. *Int J Cancer*. 2003;104:631–635.
- [15] Lyytinen I, Lempinen M, Nordin A, et al. Prognostic significance of tumor-associated trypsin inhibitor (TATI) and human chorionic gonadotropin-beta (hCGbeta) in patients with hepatocellular carcinoma. *Scand J Gastroenterol*. 2013;48:1066–1073.
- [16] Yang Y, Shi Y, Hou Y, et al. CGB5 expression is independently associated with poor overall survival and recurrence-free survival in patients with advanced gastric cancer. *Cancer Med*. 2018;7:716–725.
- [17] Kawamata F, Nishihara H, Homma S, et al. Chorionic gonadotropin-beta modulates epithelial-mesenchymal transition in colorectal carcinoma metastasis. *Am J Pathol*. 2018;188:204–215.
- [18] National Comprehensive Cancer Network (NCCN). Clinical practice guidelines in oncology. Ovarian cancer, Version 2; 2018. [cited 2018 Mar 9]. Available from: [https://www.nccn.org/professionals/physician\\_gls/pdf/ovarian.pdf](https://www.nccn.org/professionals/physician_gls/pdf/ovarian.pdf)
- [19] Voisin L, Julien C, Duhamel S, et al. Activation of MEK1 or MEK2 isoform is sufficient to fully transform intestinal epithelial cells and induce the formation of metastatic tumors. *BMC Cancer*. 2008;8:337.
- [20] Kessenbrock K, Plaks V, Werb Z. Matrix metalloproteinases: regulators of the tumor microenvironment. *Cell*. 2010;141:52–67.
- [21] Konstantinopoulos PA, Matulonis UA. Current status and evolution of preclinical drug development models of epithelial ovarian cancer. *Front Oncol*. 2013;3:296.
- [22] Decio A, Giavazzi R. Orthotopic model of ovarian cancer. *Methods Mol Biol*. 2016;1464:139–149.
- [23] Li J, Yin M, Song W, et al. B subunit of human chorionic gonadotropin promotes tumor invasion and predicts poor prognosis of early-stage colorectal cancer. *Cell Physiol Biochem*. 2018;45:237–249.
- [24] Paz H, Pathak N, Yang J. Invading one step at a time: the role of invadopodia in tumor metastasis. *Oncogene*. 2014;33:4193–4202.
- [25] Wang Y, Zhang J, Li B, et al. Proteomic analysis of mitochondria: biological and clinical progresses in cancer. *Expert Rev Proteomics*. 2017;14:891–903.
- [26] Taylor AP, Leon E, Goldenberg DM. Placental growth factor (PlGF) enhances breast cancer cell motility by mobilising ERK1/2 phosphorylation and cytoskeletal rearrangement. *Br J Cancer*. 2010;103:82–89.
- [27] Destaing O, Block MR, Planus E, et al. Invadosome regulation by adhesion signaling. *Curr Opin Cell Biol*. 2011;23:597–606.
- [28] Murphy DA, Courtneidge SA. The ‘ins’ and ‘outs’ of podosomes and invadopodia: characteristics, formation and function. *Nat Rev Mol Cell Biol*. 2011;12:413–426.
- [29] Beaty BT, Condeelis J. Digging a little deeper: the stages of invadopodium formation and maturation. *Eur J Cell Biol*. 2014;93:438–444.
- [30] Lehninger AL. Energy transformation in the cell. *Sci Am*. 1960;202:102–114.
- [31] Racker E. The membrane of the mitochondrion. *Sci Am*. 1968;218:32–39.
- [32] Giampazolias E, Tait SW. Mitochondria and the hallmarks of cancer. *FEBS J*. 2016;283:803–814.
- [33] Sotgia F, Fiorillo M, Lisanti MP. Mitochondrial markers predict recurrence, metastasis and tamoxifen-resistance in breast cancer patients: early detection of treatment failure with companion diagnostics. *Oncotarget*. 2017; 8:68730–68745.
- [34] Roskoski R Jr. ERK1/2 MAP kinases: structure, function, and regulation. *Pharmacol Res*. 2012;66:105–143.
- [35] Chakraborti S, Mandal M, Das S, et al. Regulation of matrix metalloproteinases: an overview. *Mol Cell Biochem*. 2003;253:269–285.

- [36] Li Z, Du L, Li C, et al. Human chorionic gonadotropin beta induces cell motility via ERK1/2 and MMP-2 activation in human glioblastoma U87MG cells. *J Neurooncol.* **2013**;111:237–244.
- [37] Li Z, Li C, Du L, et al. Human chorionic gonadotropin beta induces migration and invasion via activating ERK1/2 and MMP-2 in human prostate cancer DU145 cells. *PLoS One.* **2013**;8:e54592.
- [38] Wu Z, Wang T, Fang M, et al. MFAP5 promotes tumor progression and bone metastasis by regulating ERK/MMP signaling pathways in breast cancer. *Biochem Biophys Res Commun.* **2018**;498:495–501.
- [39] Guan H, Guo Z, Liang W, et al. Trop2 enhances invasion of thyroid cancer by inducing MMP2 through ERK and JNK pathways. *BMC Cancer.* **2017**;17:486.
- [40] Qin H, Liu X, Li F, et al. PAD1 promotes epithelial-mesenchymal transition and metastasis in triple-negative breast cancer cells by regulating MEK1-ERK1/2-MMP2 signaling. *Cancer Lett.* **2017**;409:30–41.
- [41] Wang JL, Yang MY, Xiao S, et al. Downregulation of castor zinc finger 1 predicts poor prognosis and facilitates hepatocellular carcinoma progression via MAPK/ERK signaling. *J Exp Clin Cancer Res.* **2018**;37:45.
- [42] Whyte J, Bergin O, Bianchi A, et al. Key signalling nodes in mammary gland development and cancer. Mitogen-activated protein kinase signalling in experimental models of breast cancer progression and in mammary gland development. *Breast Cancer Res.* **2009**;11:209.
- [43] Nwabuobi C, Arlier S, Schatz F, et al. hCG: biological functions and clinical applications. *Int J Mol Sci.* **2017**;18(10):E2037.
- [44] Keryer G, Alsat E, Tasken K, et al. Cyclic AMP-dependent protein kinases and human trophoblast cell differentiation *in vitro*. *J Cell Sci.* **1998**;111(Pt 7):995–1004.
- [45] Lu JJ, Zheng Y, Kang X, et al. Decreased luteinizing hormone receptor mRNA expression in human ovarian epithelial cancer. *Gynecol Oncol.* **2000**;79:158–168.
- [46] Jankowska A, Andrusiewicz M, Grabowski J, et al. Coexpression of human chorionic gonadotropin beta subunit and its receptor in nontrophoblastic gynecological cancer. *Int J Gynecol Cancer.* **2008**;18:1102–1107.
- [47] Mandai M, Konishi I, Kuroda H, et al. LH/hCG action and development of ovarian cancer—a short review on biological and clinical/epidemiological aspects. *Mol Cell Endocrinol.* **2007**;269:61–64.
- [48] Glodek A, Jankowska A. CGB activates ERK and AKT kinases in cancer cells via LHCGR-independent mechanism. *Tumour Biol.* **2014**;35:5467–5479.
- [49] Szczerba A, Sliwa A, Kubiczak M, et al. Human chorionic gonadotropin beta subunit affects the expression of apoptosis-regulating factors in ovarian cancer. *Oncol Rep.* **2016**;35:538–545.